

DETERMINING FORMING LIMIT CURVES USING DIC

Sheet metal forming is a key manufacturing technology in modern mechanical engineering, used to produce thin-walled components with high dimensional accuracy and tailored mechanical properties. As industries strive for lighter and more efficient structures, accurately defining the formability limits of sheet metal blanks has become increasingly important.

These limits are typically represented by Forming Limit Diagrams (FLDs), which illustrate how the material behaves under different combinations of stretching and compression. They make it possible to predict when and where the material will fail during forming. To determine these limits experimentally, engineers often use the Nakajima test, in which specimens are subjected to various stress states until fracture.

This project, conducted as part of a student thesis, involved the design and validation of a custom test fixture in full compliance with ISO 12004-2. The deformation of the specimens during loading was measured using stereoscopic (3D) Digital Image Correlation (DIC), a noncontact optical method that provides highly precise, full-field strain data.



KEY WORDS

- Nakajima Test
- Digital Image Correlation
- Forming limit curve (FLC)
- Forming limit diagram (FLD)
- ČSN EN ISO 12004-2

TEST SETUP

- 3D DIC System
- Hydraulic press DR 520 CA
- Stochastic pattern kit
- Alpha DIC software tools:
 - DIC Area
 - Point probe
 - Bend Line
 - 。 FI C
 - Post process

OUTPUT

- Forming Limit Diagram
- Section Analysis
- Major-Minor Strain Behaviour



SPECIMENS AND MEASUREMENT SETUP

Before measurement, a set of metallic sheet specimens made from DR 520 CA with a nominal thickness of 0.2 mm was prepared. The aim was to generate various stress states during the Nakajima-type forming test. To achieve this, geometrically distinct specimens were designed (see Fig. 2), comprising:

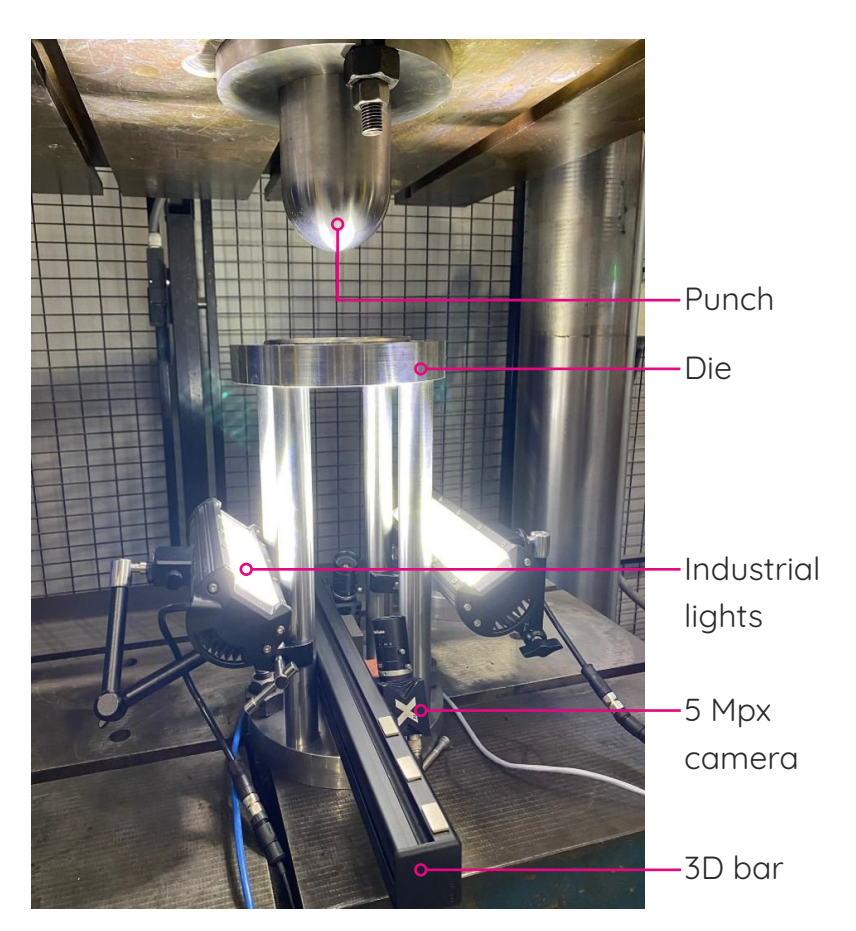
- Flat specimens (strips) with widths of 40 mm, 50 mm, 60 mm, 70 mm, and 90 mm
- Circular specimens with a diameter of 155 mm



▲ Figure 2 : Geometry of the test specimens

Each specimen geometry was manufactured in three identical pieces to ensure repeatability and allow statistical evaluation of the test results. The forming tests were carried out using a custom experimental fixture designed for compatibility with the Digital Image Correlation (DIC) method, which integrates all standard forming components, including a punch, die, drawbead, and blank holder. In addition, vertical spacers were incorporated to elevate the tooling assembly, providing a clear optical path for the DIC system positioned beneath the specimen.

The complete fixture was installed on a CBJ 500-6 hydraulic press, which supplied the required forming force. Following the mechanical setup, the X-Sight 3D DIC system was deployed. The entire measurement process was controlled and evaluated using the X-Sight Alpha DIC software. A full view of the prepared measurement setup is shown in Fig. 3.





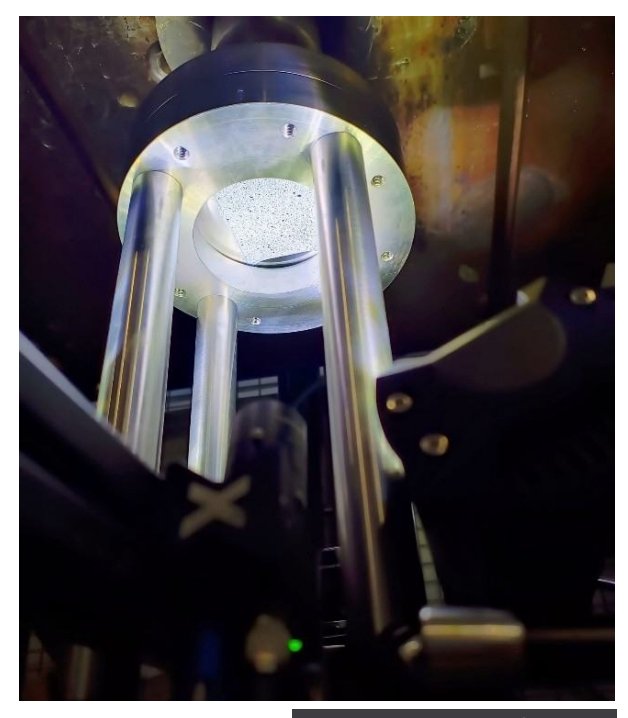
◀ ▲ Figure 3,4: Measurement set-up, measurement scene

MFASIIRFMFNT

Before testing, a thin layer of lubricant was applied to both the specimen surface and the hemispherical punch to reduce friction, promote smoother deformation, and minimize the risk of surface damage. In addition, the DIC system was calibrated prior to measurement.

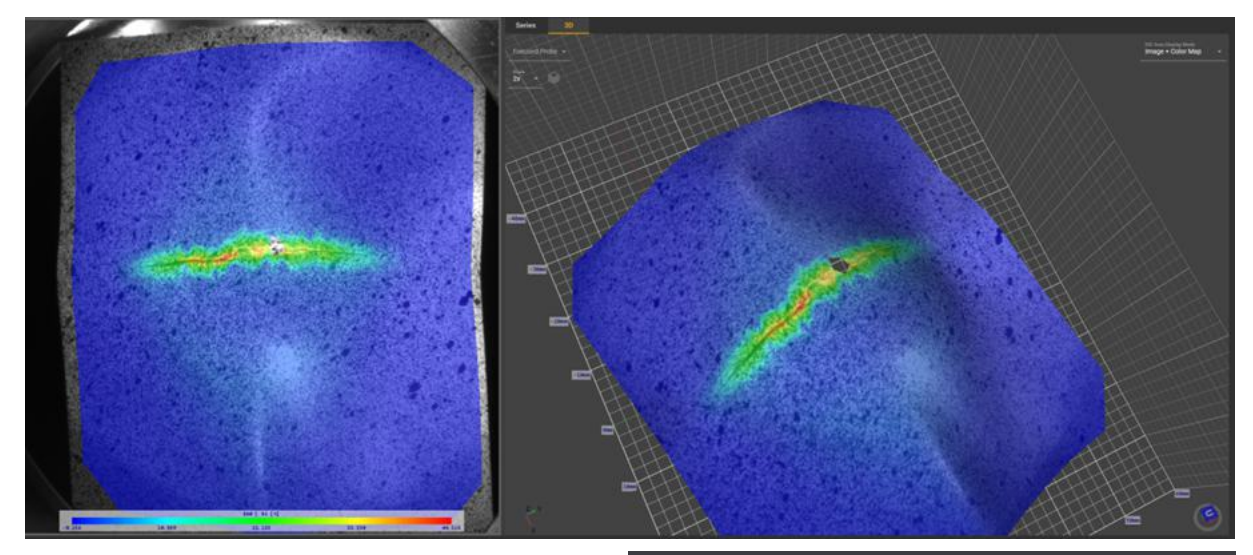
At the beginning of the testing phase, each specimen was carefully positioned on the drawbead support of the forming fixture and secured with the blank holder. To ensure uniform clamping pressure, two temporary spacers were inserted between the upper fixture plate and the blank holder, which was then lightly tightened with four screws to achieve preliminary contact with the specimen. Afterwards, the spacers were removed and the blank holder was fully tightened using four additional screws. All fasteners were torqued in a cross pattern to prevent distortion or asymmetric loading, ensuring stable and repeatable specimen fixation (Fig. 5).

The forming process began with the punch moving downward, gradually applying pressure to the specimen to simulate realistic sheet metal forming conditions. Throughout the deformation, the X-Sight stereoscopic DIC system continuously recorded the full-field 3D displacement and strain evolution.



▲ Figure 5: Set-up ready for testing

The test was terminated at the onset of material failure, as detected in the Alpha DIC software (see Fig. 6), which was defined by the appearance of a crack in the specimen. After fracture, the specimen was carefully removed and stored for post-test evaluation. This procedure was repeated for all specimens to ensure repeatable and consistent results across the entire test series.

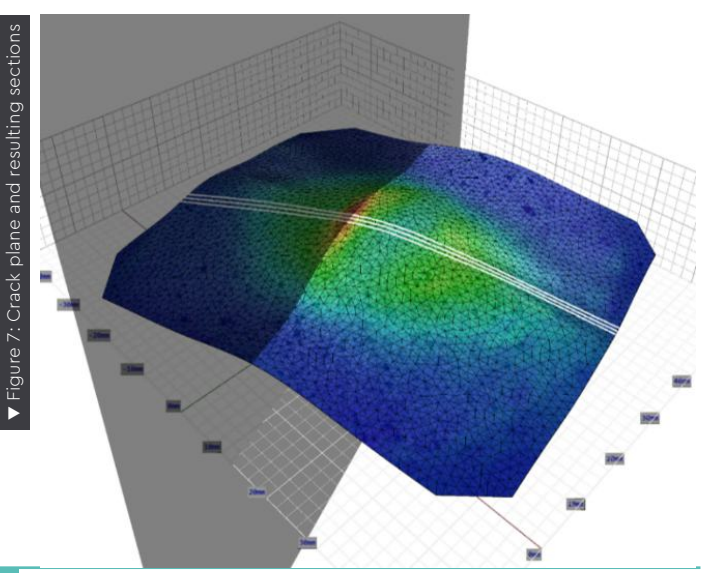


MEASUREMENT EVALUATION

This section presents the evaluation of data obtained from experimental measurements. For clarity, a single representative specimen—sample 70a, corresponding to a strip with a width of 70 mm—was selected. The complete evaluation procedure is demonstrated on this specimen.

The analysis was performed in Alpha DIC using its basic post-processing tools and the Forming Limit Curve (FLC) module for advanced evaluation. This module enables detailed section-based analysis in full compliance with ISO 12004-2 (see Fig. 7).

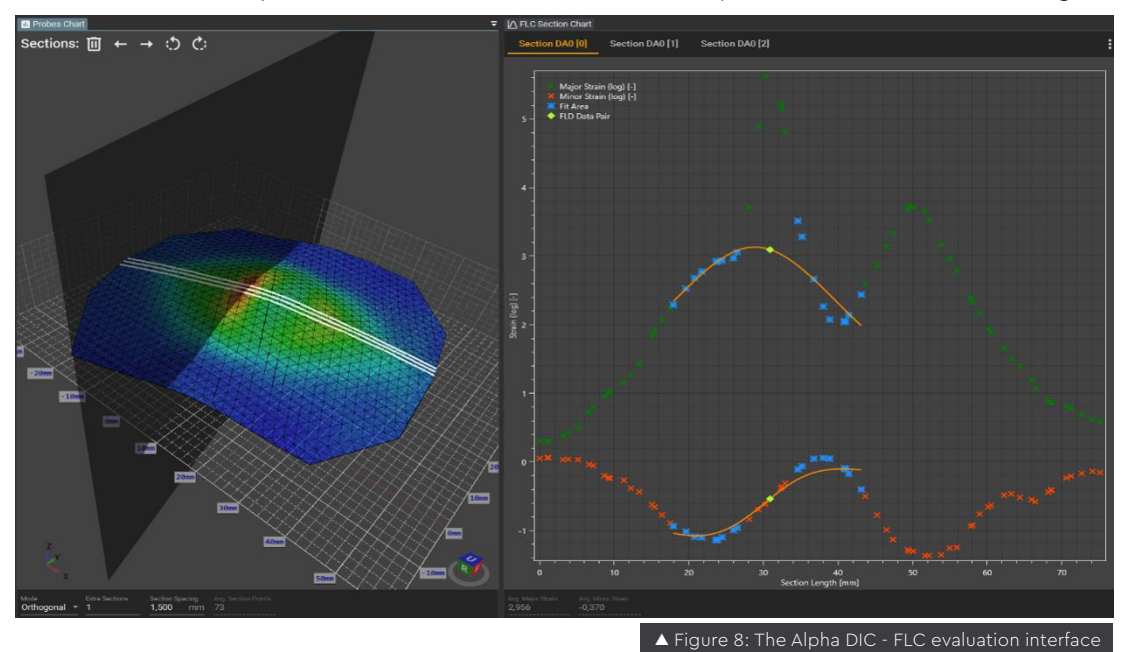
▲ Figure 6: Material failure visible in Alpha DIC at the end of the test



At the location of failure—typically visible in the strain map as a red-colored region indicating maximum strain—a measurement plane was positioned and oriented along the crack direction. Perpendicular to this plane, three centerlines were defined, each representing a conceptual cross-sectional cut through the crack area. Along each centerline, the software automatically evaluated the strain distribution, from which the major and minor engineering strain values (ϵ_1 , ϵ_2) were extracted. These strain values were then converted to true (logarithmic) strains (ϕ_1 , ϕ_2), as required for constructing the FLCs. Additional sections could be added for further evaluation if necessary.

The evaluation was conducted at two critical time points: immediately prior to crack initiation and after crack initiation. This dual-point analysis was selected because the primary goal of these tests was to support the development of an advanced material model for forming simulations, which requires an in-depth evaluation of the material behavior.

The FLC module also allows the user to apply an automatic polynomial fit (see Fig. 8), which significantly accelerates the evaluation process. However, this approach involves the use of a safety coefficient and therefore does not represent the true material limits required for material model development. For this reason, the maximum measured values from both evaluation time points were used in the material model, as described in the following sections.

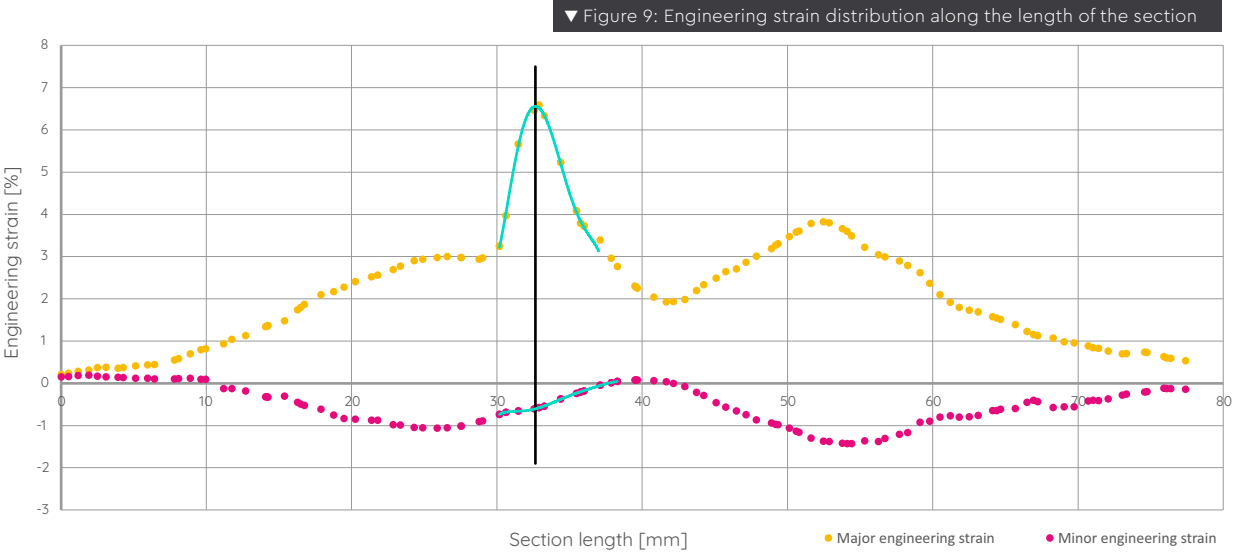


AFTER CRACK INITIATION EVALUATION

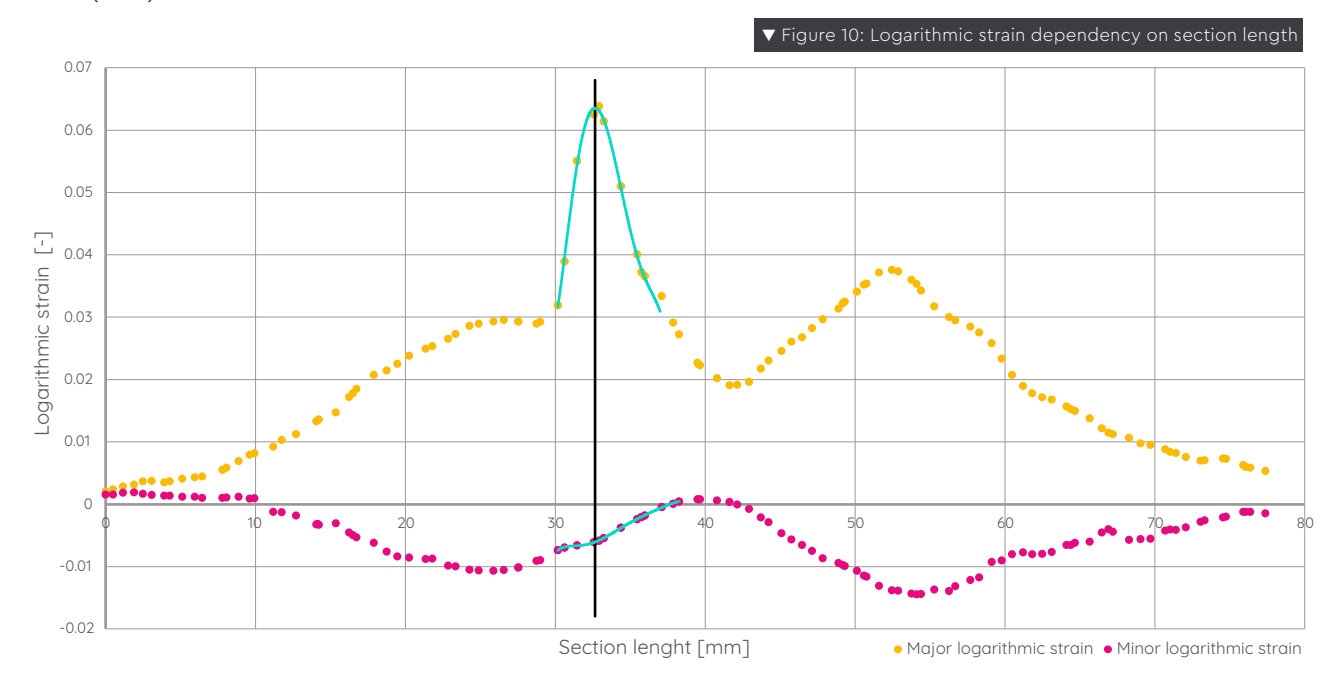
Figure 9 corresponds to the middle centerline and shows the engineering strain profile along the section cut through the crack area. Two data curves are presented:

- The yellow curve represents the distribution of major strain.
- The pink curve shows the distribution of minor strain.

The crack center is marked by a vertical black line, indicating the location of maximum strain, which corresponds to the material's limit point. In accordance with ISO 12004-2, a smoothing polynomial regression was applied to the strain data near the crack zone (green curve in Fig. 10), enabling a more precise determination of the local maximum of major strain. Its intersection with the vertical black line defines this maximum and the corresponding minor strain value.



To provide a complete view of the deformation state, Figure 10 presents an equivalent graph constructed using the logarithmic (true) strain.



Strain values extracted from all tested specimens, summarized in Table 1, were used to construct the FLC representing the boundary between safe deformation and material failure.

Specimen no.	$\epsilon_{\scriptscriptstyle 1}$	$oldsymbol{\epsilon_2}$	φ1	ϕ_2
40a	8,391	-0,845	0,0806	-0,0085
40b	8,386	-0,836	0,0805	-0,0084
40c	8,379	-0,857	0,0805	-0,0086
50a	5,303	-0,167	0,0517	-0,0017
50b	5,294	-0,147	0,0516	-0,0015
50c	5,311	-0,155	0,0517	-0,0016
60a	8,309	-0,841	0,0798	-0,0084
60b	8,292	-0,828	0,0797	-0,0083
60c	8,301	-0,835	0,0797	-0,0084
70a	6,584	-0,608	0,0638	-0,0061
70b	6,558	-0,589	0,0635	-0,0059
70c	6,602	-0,614	0,0639	-0,0062
90a	5,305	-0,407	0,0517	-0,0041
90b	5,320	-0,417	0,0518	-0,0042
90c	5,286	-0,394	0,0515	-0,0039
155a	21,308	7,188	0,1932	0,0694
155b	21,277	7,215	0,1929	0,0697
155c	21,322	7,235	0,1933	0,0699

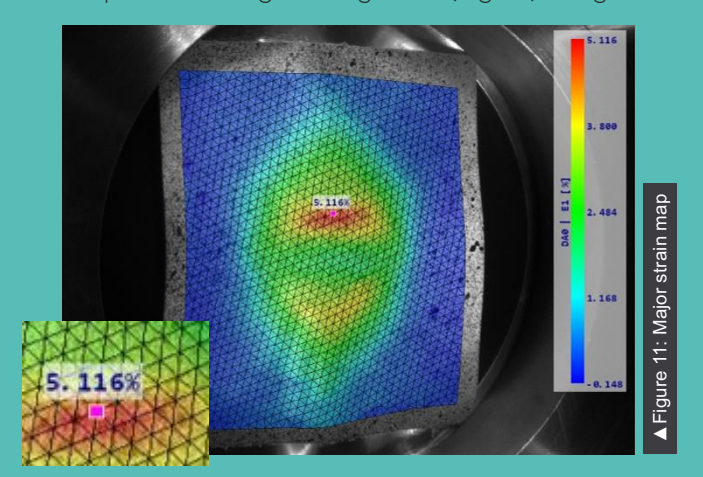
lack lack Table 1: Engineering and logarithmic values of evaluated specimens (After crack initiation)

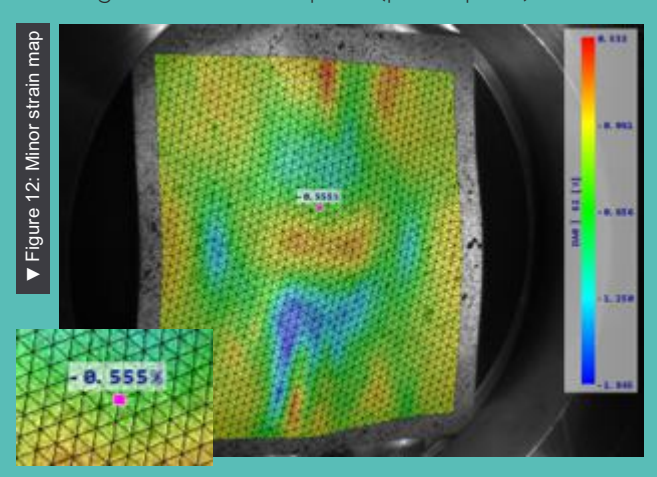
BEFORE CRACK INITIATION EVALUATION

To determine the material's limit state, a single frame from each test series was selected—captured immediately before failure. This frame represents the critical condition corresponding to the highest material stress.

The evaluation was performed in the Alpha DIC software using the color map of major engineering strain. A pink-marked point (Figs. 11 and 12) in the region of the future crack identified the global maximum of major strain (ε_1 = 5.116%) in both the strain map and the section diagram within the FLC evaluation interface. This point was located within the red deformation zone (Fig. 11), approximately 4 mm from the specimen center.

Unlike the major strain, which typically peaks directly at the crack center, the global maximum of minor strain ($\varepsilon_{2,max} = -1.845\%$) occurred in a blue-colored area unrelated to the actual failure location. Therefore, its evaluation had to be carefully focused on the crack initiation site to ensure that the resulting strain pair (ε_1 , ε_2) reflected the material's true limit state and could be used to construct the FLC. The corresponding value ($\varepsilon_2 = -0.555\%$) was thus obtained from the map of minor engineering strain (Fig. 12) using the same mesh settings and evaluation point (pink square).





All specimens were analyzed using this procedure—first identifying the local maximum of the major strain (ϵ_1), and then determining the corresponding minor strain (ϵ_2) at the same location within the future crack region. The engineering strain pairs were subsequently converted to logarithmic strains, denoted as ϕ_1 and ϕ_2 . A complete overview of all obtained values is provided in Table 2.

Specimen no.	ε ₁	\mathcal{E}_2	φ1	φ ₂
40a	6,569	-0,820	0,0636	-0,0082
40b	6,586	-0,815	0,0638	-0,0082
40c	6,519	-0,829	0,0632	-0,0083
50a	5,219	-0,497	0,0509	-0,0050
50b	5,158	-0,513	0,0503	-0,0051
50c	5,285	-0,479	0,0515	-0,0048
60a	5,068	-0,461	0,0494	-0,0046
60b	4,978	-0,475	0,0486	-0,0048
60c	5,181	-0,457	0,0505	-0,0046
70a	5,116	-0,555	0,0499	-0,0056
70b	5,209	-0,539	0,0508	-0,0054
70c	5,092	-0,561	0,0497	-0,0056
90a	4,840	-0,207	0,0473	-0,0022
90b	4,901	-0,218	0,0478	-0,0021
90c	4,779	-0,205	0,0467	-0,0022
155a	14,764	8,138	0,1377	0,0782
155b	14,821	8,255	0,1382	0,0793
155c	14,747	8,201	0,1376	0,0788

▲ Table 2: Engineering and logarithmic values of evaluated specimens (before crack initiation)

BEFORE CRACK INITIATION EVALUATION

The FLD was first constructed using engineering strains, as shown in Figure 13. In this graph, pink points represent strain values obtained immediately after specimen failure. These points were fitted with two distinct functions:

- a polynomial function on the left side of the diagram, and
- a linear function on the right side.

The resulting green curve defines the FLC of the material — a boundary beyond which permanent material damage occurs.

An identical approach was applied to the data from the pre-fracture phase, shown as yellow points. Fitting these data points produced the grey curve, which represents the FLC for the state of the material without visible failure.

Both curves were verified using the calculated reference point $FLC_{10} = 4.6\%$, representing the uniaxial tensile state ($\epsilon_2 = 0$) and marked in the diagram with a red triangle. Their close intersection near this point confirms the validity of the experimental and analytical procedures, demonstrating that the results accurately reflect the material's true behavior and comply with the applicable international standard.

Figure 14 shows the equivalent FLD constructed in the same way using logarithmic strains from Tables 1 and 2, and the reference point $FLC_{20} = 0.045$.

